Halterman Corroles and Their Application to an Investigation of the Conformational Dynamics of the Inherently Chiral Copper Corrole Chromophore

Kolle E. Thomas,[a] Laura J. McCormick,[b] Daniel Carrié,[c] Hugo Vazquez-Lima,[a]
Gérard Simonneaux,*[,c] and Abhik Ghosh*[,a]

[a]Department of Chemistry, UiT – The Arctic University of Norway, N-9037 Tromsø, Norway;
[b]Advanced Light Source, Lawrence Berkeley National Laboratory,
Berkeley, CA 94720-8229, USA
[c]Institut des Sciences Chimiques de Rennes UMR 6226 Université de Rennes 1 Campus de Beaulieu 35042 Rennes, France

Email: gerard.simonneaux@univ-rennes1.fr (GS), abhik.ghosh@uit.no (AG)

Abstract. Halterman corroles have been synthesized for the first time from pyrrole and Halterman's aldehyde via Gryko's "water-methanol method". These were derivatized to the corresponding copper complexes and subsequently also to the β-octabromo complexes. Electronic circular dichroism spectra were recorded for the enantiopure copper complexes, affording the first such measurements for the inherently chiral Cu corrole chromophore. Interestingly, for a given configuration of the Halterman substituents, X-ray crystallographic studies revealed both *P* and *M* conformations of the Cu-corrole core, proving that the substituents, even in conjunction with β-octabromination, are unable to lock the Cu-corrole core into a given chirality. The overall body of evidence strongly indicates a dynamic equilibrium between the *P* and *M* conformations. Such an interconversion, which presumably proceeds via saddling inversion, provides a rationale for our failure so far to resolve sterically hindered Cu corroles into their constituent enantiomers by means of chiral HPLC.

Note: The crystal structures described in this paper have been deposited at the Cambridge Crystallographic Data Centre and been assigned the following deposition numbers: CCDC 1576180-1576182.

Introduction. The concept of an *inherently chiral* chromophore was first introduced by Moscowitz and others over a half-century ago[1,2] and refers to molecular systems whose chirality cannot be ascribed to classic stereogenic elements, in particular stereogenic centers.[3] Of particular interest from the point of view of chiroptical properties are inherently chiral chromophores with curved π-systems such as helicenes[4] and certain fullerenes (e.g. D_2-C_{76}, D_3-C_{78}, D_2-C_{80}, and D_2-C_{84}).[5] In the course of our own research on the coordination chemistry of corroles,[6] we have discovered two different classes of inherently chiral chromophores. The first of these to be discovered, copper corroles, owe their chirality to an electronically driven saddling of the macrocycle, which allows an otherwise symmetry-forbidden Cu(d_{x2-y2})-corrole(π) orbital interaction.[7,8,9,10,11] Steric crowding due to peripheral substituents can accentuate this saddling, but steric effects alone, in the absence of the electronic imperative, do not bring about saddling of the macrocycle.[12] To our disappointent, so far we have not been able to resolve Cu corroles; chiral HPLC experiments have failed to resolve even highly saddled copper *β*-octabromo-[13,14] and *β*-octakis(trifluoromethyl)-[15,16] *meso*-triarylcorroles.[17] In contrast, a second class of inherently chiral metallocorroles, Mo[18] and W[19] biscorroles, have been successfully resolved and the enantiomers of a W biscorrole have been chracterized via electronic circular dichroism spectroscopy.[17,20]

Herein, we have revisited the challenge of synthesizing copper corroles in enantiomerically pure or enriched form by appending chiral substituents on the corrole periphery. Toward that end, we synthesized the corrole analogue of a Halterman porphyrin via the oxidative condensation of enantiopure 1,2,3,4,5,6,7,8-octahydro-1:4,5:8-dimethanoanthracene-9-carboxaldehyde (hereafter referred to as $\mathcal{H}$-CHO, where $\mathcal{H}$ refers to the Halterman substituent of either chirality) and pyrrole.[21,22] A modified version of Gryko's water-methanol method,[23] employing higher dilutions (to solubilize the relatively nonpolar aldehyde) and longer reaction times (16-18 h), led to good yields (~40%) of the Halterman corroles (Figure 1). Copper was then inserted and the Cu complexes *β*-octabrominated with elemental bromine via standard protocols.[7] Single-crystal X-ray structures were successfully obtained for three different Cu[$\mathcal{H}_3$Cor] (Cor = corrole) derivatives. As discussed below, the structures clearly showed that the Halterman substituents in conjunction with *β*-octabromo-substitution are unable to lock the Cu-corrole conformation into a given chirality, which may be described by a *P*/*M* nomenclature as illustrated in Figure 2. The chemical implications of these findings are also discussed below.

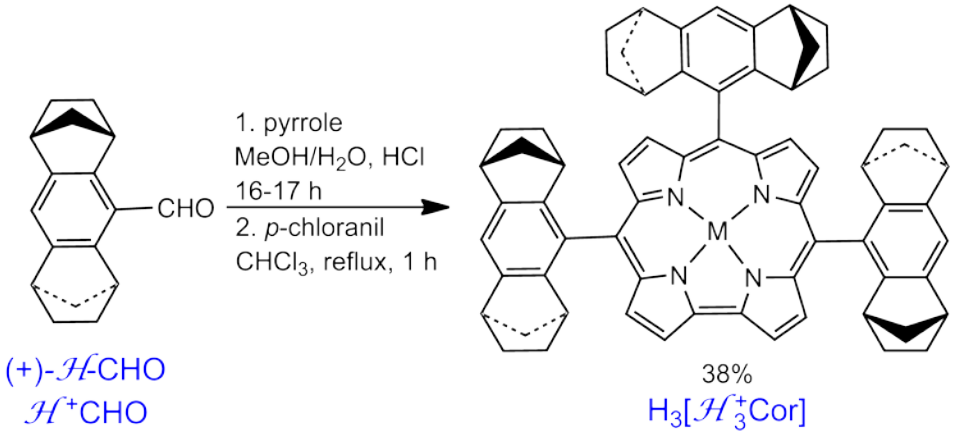

Figure 1. Synthesis of a Halterman corrole, where $\mathcal{H}^{+}$ denotes the (1*S*,4*R*,5*R*,8*S*)-1,2,3,4,5,6,7,8-octahydro-1:4,5:8-dimethanoanthracen-9-yl substituent, which occurs in the (+)-isomer of the Halterman aldehyde; $\mathfrak{R}$ denotes the same substituent of either chirality.

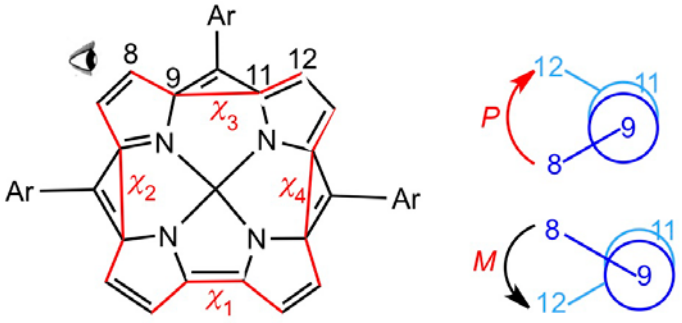

Figure 2. Definition of saddling torsion angles (χ_1- χ_4). The inherent chirality of Cu corroles is defined here in terms of the sign of the C_8-C_9-C_{11}-C_{12} (χ_3) torsion angle.

Results and discussion. Table 1 presents crystal and refinement data for the three single-crystal structures reported herein and Tables 2-4 present selected distances, angles, and torsion angles. In general, these structural parameters are similar to those of related Cu corrole structures reported in the literature. Some of the more notable aspects of the structures are as follows.H

The X-ray structure of enantiopure Cu[$\mathcal{H}^{+}_3$Cor] (Figure 3 and Table 2) shows that all corrole units are identical and may be described as relatively mildly saddled, with only one moderately large saddling dihedral at ~38°. The $\mathcal{H}^{+}$ substituents have led to a uniform *P* configuration of the Cu-corrole ring system. In contrast, the enantiopure *β*-octabrominated

complex Cu[Br$_8$$\mathcal{H}^-_3$Cor] was found to contain two stereochemically distinct Cu[Br$_8$$\mathcal{H}^-_3$Cor] units, one with *M* and the other with *P* configuration, both of which exhibit a strongly saddled Cu-corrole core with saddling dihedrals in the range 47-68°. There is some positional disorder involving the 10-$\mathcal{H}^-$ group of the *P*-Cu[Br$_8$$\mathcal{H}^-_3$Cor] unit; however, the enantiopurity of the molecule is not in question.

Table 1. Crystal and refinement data for Cu Halterman corroles.

Sample	Cu[$\mathcal{H}^+_3$Cor]	Cu[Br$_8$$\mathcal{H}^-_3$Cor]	Cu[Br$_8$-5,15-$\mathcal{H}^\pm_2$-10-$\mathcal{H}^\mp$Cor]
Chemical Formula	$C_{69}H_{63}Cl_4CuN_4$	$C_{73.75}H_{66.56}Br_8Cl_{0.41}CuN_4$	$C_{77.74}H_{75.31}Br_8Cl_{1.71}CuN_4$
Formula mass	1153.57	1726.20	1828.90
Crystal system	Orthorhombic	Monoclinic	Monoclinic
Space group	$P2_12_12_1$	$C2$	$C2/c$
λ (Å)	0.7749	0.7749	0.7749
a (Å)	11.8437(6)	11.5580(6)	11.4727(6)
b (Å)	17.9042(9)	23.9229(12)	23.9890(12)
c (Å)	26.3407(13)	25.9436(13)	25.9406(13)
α (°)	90	90	90
β (°)	90	91.359(2)	91.002(3)
γ (°)	90	90	90
Z	4	4	4
V (Å^3)	5585.6(5)	7171.4(6)	7138.2(6)
Temperature (K)	100(2)	100(2)	100(2)
ρ (g/cm^3)	1.372	1.599	1.702
Measured reflections	386855	428802	40786
Unique reflections	23535	28900	8921
Parameters	703	843	391
Restraints	0	122	84
R_{int}	0.0549	0.0618	0.0713
Abs. struct. parameter	0.0300(14)	0.028(3)	-
θ range (°)	1.499 to 38.123	0.856 to 37.450	1.712 to 31.276
*R*1, *wR*2 all data	0.0475, 0.1322	0.0397, 0.0929	0.0713, 0.1341
S (*GooF*) all data	1.085	1.052	1.109
Max/min res. Dens. (e/Å^3)	1.242/-1.653	1.114/-1.463	1.459/-1.119

Table 2. Selected distances (Å), angles (°), and torsion angles (°) for Cu[$\mathcal{H}^{+}_{3}$Cor].

Distances		*Angles*	
N(1)-Cu(1)	1.8681(19)	N(1)-Cu(1)-N(4)	81.74(9)
N(2)-Cu(1)	1.8808(18)	N(1)-Cu(1)-N(3)	169.48(9)
N(3)-Cu(1)	1.8798(18)	N(4)-Cu(1)-N(3)	91.74(8)
N(4)-Cu(1)	1.879(2)	N(1)-Cu(1)-N(2)	90.68(8)
		N(4)-Cu(1)-N(2)	167.66(9)
		N(3)-Cu(1)-N(2)	97.08(8)

Torsion angles	
C(3)-C(4)-C(6)-C(7)	-16.9(8)
C(8)-C(9)-C(11)-C(12)	22.4(7)
C(13)-C(14)-C(16)-C(17)	-38.3(8)
C(18)-C(19)-C(1)-C(2)	16.8(6)

Table 3. Selected distances (Å), angles (°), and torsion angles (°) for Cu[$Br_8\mathcal{H}^{-}_{3}$Cor].

Distances		*Angles*	
Cu(1)-N(1)	1.910(3)	N(1)-Cu(1)-N(1)^{I}	82.5(2)
Cu(1)-N(2)	1.914(3)	N(1)-Cu(1)-N(2)^{I}	168.88(17)
Cu(2)-N(101)	1.915(3)	N(1)-Cu(1)-N(2)	90.71(15)
Cu(2)-N(102)	1.915(3)	N(2)^{I}-Cu(1)-N(2)	97.3(2)
		N(101)^{II}-Cu(2)-N(101)	82.92(19)
		N(101)-Cu(2)-N(102)	90.56(13)
		N(101)^{II}-Cu(2)-N(102)^{II}	90.57(13)
		N(101)-Cu(2)-N(102)^{II}	168.49(14)
		N(102)-Cu(2)-N(102)^{II}	97.35(19)

Torsion angles	
C(3)-C(4)-C(6)-C(7)	67.4(15)
C(8)-C(9)-C(9)^{I}-C(8)^{I}	-59(2)
C(2)-C(1)-C(1)^{I}-C(2)^{I}	-51.0(14)
C(103)-C(104)-C(106)-C(107)	-67.6(11)
C(108)-C(109)-C(109)^{II}-C(108)^{II}	50.2(15)
C(102)-C(101)-C(101)^{II}-C(102)^{II}	47.4(12)

Symmetry transformations used to generate equivalent atoms:

I: -x+1, y, -z **II:** -x+1, y, -z+1

Table 4. Selected distances (Å), angles (°), and torsion angles (°) for Cu[$Br_8$5,15-$\mathcal{H}^{\mp}_2$-10-$\mathcal{H}^{\mp}$Cor].

Distances	*Angles*	
N(1)-Cu(1) 1.906(4)	N(1)-Cu(1)-N(1)^{I}	82.5(2)
N(2)-Cu(1) 1.921(4)	N(1)-Cu(1)-N(2)	91.02(17)
	N(1)-Cu(1)-N(2)^{I}	168.95(19)
	N(2)-Cu(1)-N(2)^{I}	96.7(2)
Torsion angles		
C(3)-C(4)-C(6)-C(7)	-63.0(18)	
C(8)-C(9)-C(9)#1-C(8)#1	57(2)	
C(2)-C(1)-C(1)#1-C(2)#1	47.9(16)	

Symmetry transformations used to generate equivalent atoms:

I: -x+1, y, -z+1/2

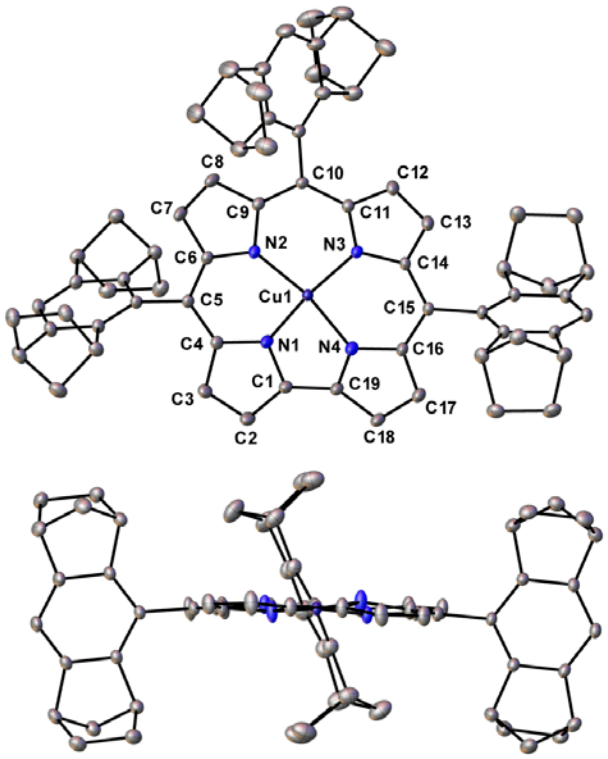

Figure 3. Top and side views of the X-ray structure of Cu[$\mathcal{H}^{+}_3$Cor]. Thermal ellipsoids for this and all subsequent figures are shown at 50% probability.

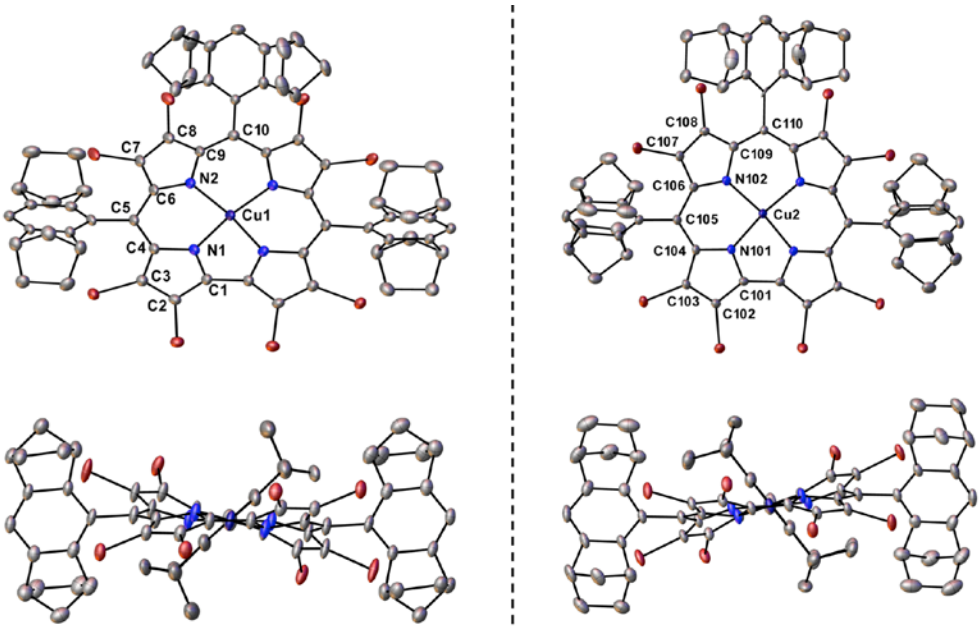

Figure 4. X-ray structure of Cu[$Br_8\mathcal{H}_3$Cor] containing an equimolar distribution of the *P* (left) and *M* (right) conformations. The thermal ellipsoids have been drawn at 50% probability.

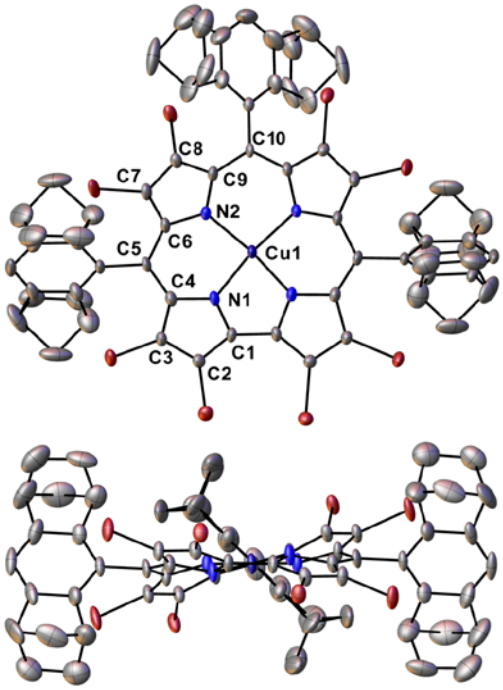

Figure 5. Top and side views of the molecular structure of racemic Cu[Br_8-5,15-$\mathcal{H}^{\pm}_2$-10-$\mathcal{H}^{\mp}$Cor]. The molecule shown is the *P*-Cu[$Br_8$5,15-$\mathcal{H}_2$-10-$\mathcal{H}^{+}$Cor] enantiomer and, for clarity, only the major orientation of the $\mathfrak{R}$ groups are shown. The thermal ellipsoids have been drawn at 50% probability.

X-ray analysis revealed that the use of (±)-$\mathcal{H}$-CHO in the corrole synthesis and subsequent bromination leads almost exclusively to Cu[Br_8-5,15-$\mathcal{H}^{\pm}_2$-10-$\mathcal{H}^{\mp}$Cor] (i.e., a diastereomer of Cu[$Br_8\mathcal{H}^{+}_3$Cor]/Cu[$Br_8\mathcal{H}^{-}_3$Cor]), in which the Halterman substituent at the 10-position has a different chirality relative to the 5- and 15-substituents (Figure 5 and Table 3). Not surprisingly, the two diastereomeric structures – Cu[$Br_8\mathcal{H}^{-}_3$Cor] and Cu[$Br_8$5,15-$\mathcal{H}^{\pm}_2$-10-$\mathcal{H}^{\mp}$Cor] – were found to be very similar in terms of key structural parameters such as Cu-N distances and saddling dihedrals. Also, as in the case of Cu[$Br_8\mathcal{H}^{-}_3$Cor], the crystal structure of racemic Cu[$Br_8$5,15-$\mathcal{H}^{\pm}_2$-10-$\mathcal{H}^{\mp}$Cor] revealed evidence of conformational multiplicity for both enantiomers. Thus, all three $\mathcal{H}$ groups on a given molecule were found to exhibit a small amount (~14%) of disorder, indicating that although a majority of the Cu-corrole units in the Cu[Br_8-5,15-$\mathcal{H}^{-}_2$-10-$\mathcal{H}^{+}$Cor] enantiomer exhibits a *P* conformation, a small proportion of the molecules (~14%) exhibits an *M* conformation. Obviously, analogous observations apply for the other enantiomer.

The enantiopure products Cu[$\mathcal{H}^{+}_3$Cor]/Cu[$\mathcal{H}^{-}_3$Cor] and Cu[$Br_8\mathcal{H}^{+}_3$Cor]/Cu[$Br_8\mathcal{H}^{-}_3$Cor] were also characterized via electronic circular dichroism (ECD) spectroscopy (Figure 6). The key spectral features clearly correspond to the Soret and Q bands of the complexes, indicating that they arise largely from the Cu-corrole moiety and not from the substituents. Observable ECD spectra also strongly suggest that the *P* and *M* conformations are present in unequal amounts in solution, in contrast to the 1:1 *P*/*M* ratio found in the X-ray structure of Cu[$Br_8\mathcal{H}^{-}_3$Cor], implying a dynamic equilibrium between the *P* and *M* conformations in solution. Such a conclusion is also in accord with DFT calculations (Table 4), which indicate exceedingly small energy differences between the *P* and *M* conformations for all the molecules studied. Unfortunately, extensive signal overlap precluded a ^{1}H NMR analysis of the *P*/*M* equilibrium.

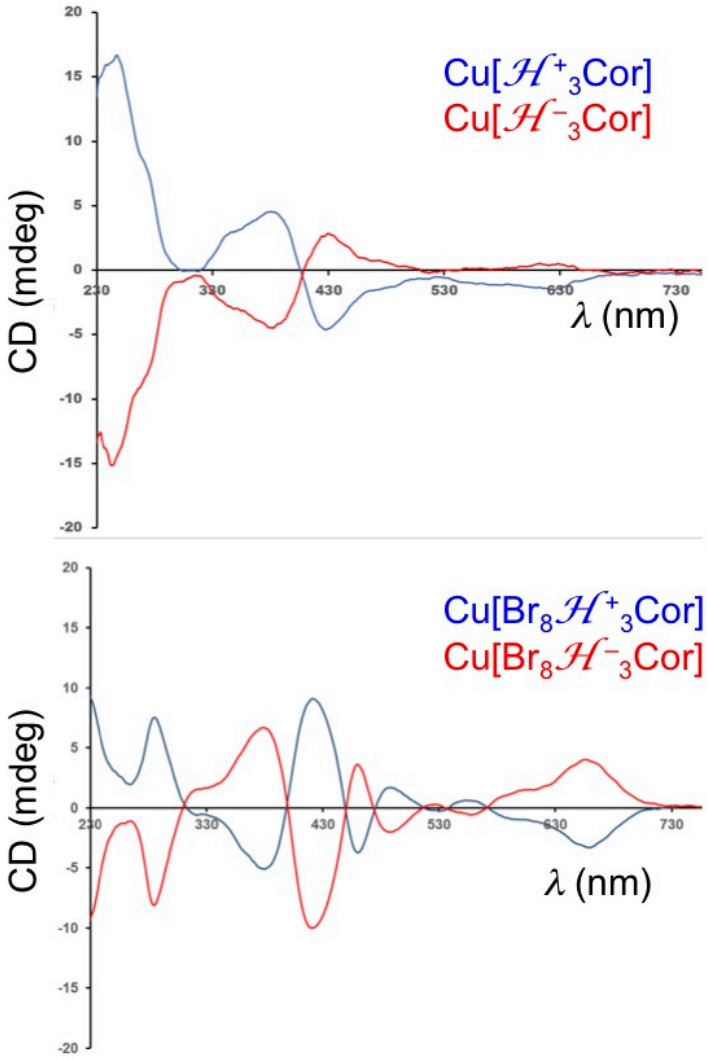

Figure 6. Circular dichroism spectra of Cu[$\mathcal{H}^{+}_{3}$Cor]/Cu[$\mathcal{H}^{-}_{3}$Cor] and Cu[$Br_8\mathcal{H}^{+}_{3}$Cor]/ Cu[$Br_8\mathcal{H}^{-}_{3}$Cor].

Table 4. OLYP/TZ2P relative energetics (eV) and saddling dihedrals (°).

			Saddling dihedral[a]		
Molecule	Conformation	E_{rel}	χ_1	χ_2/χ_4	χ_3
Cu[$\mathcal{H}^{+}_3$Cor]	P	0.094	25.5	-42.1	33.4
			16.8(6)	**-16.9(8)/-38.3(8)**	**22.4(7)**
Cu[$\mathcal{H}^{+}_3$Cor]	*M*	0.023	-24.1	42.2	-33.5
Cu[5,15-$\mathcal{H}^{+}_2$-10-$\mathcal{H}^{-}$Cor]	*P*	0.120	26.5	-43.4	36.0
Cu[5,15-$\mathcal{H}^{+}_2$-10-$\mathcal{H}^{-}$Cor]	*M*	0.000	-23.0	41.4	-33.9
Cu[Br$_8\mathcal{H}^{+}_3$Cor]	*P*	0.081	50.1	-69.4	64.8
			47.4(12)	**-67.6(11)**	**50.2(15)**
Cu[Br$_8\mathcal{H}^{+}_3$Cor]	*M*	0.018	-49.6	69.1	-62.9
			-51.0(14)	**67.4(15)**	**-59(2)**
Cu[Br$_8$5,15-$\mathcal{H}^{+}_2$-10-$\mathcal{H}^{-}$Cor]	*P*	0.101	50.0	-68.6	63.8
			47.9(16)	**-63.0(18)**	**57(2)**
Cu[Br$_8$5,15-$\mathcal{H}^{+}_2$-10-$\mathcal{H}^{-}$Cor]	*M*	0.000	-48.8	68.3	-63.7

* The values in bold have been obtained from the crystallographic structures.

It is worth noting that the calculated energetics does not offer any insights into why racemic $\mathcal{H}$-CHO should selectively afford the H$_3$[5,15-$\mathcal{H}^{\pm}_2$-10-$\mathcal{H}^{\mp}$Cor] diastereomer as opposed to H$_3$[$\mathcal{H}^{+}_3$Cor]/H$_3$[$\mathcal{H}^{-}_3$Cor]. A comparison of the relative energies of the corresponding Cu complexes (in their lowest-energy conformations) proved unenlightening, since they are essentially identical.

Conclusion. In summary, the first Halterman corrole ligand has been synthesized in reasonably good yield and derivatized to the corresponding copper and β-octabrominated copper derivatives. Access to an enantiomeric excess of the inherently chiral Cu-corrole chromophore in solution has allowed the determination of its electronic circular dichroism spectrum for the first time. Single-crystal X-ray structures were obtained for three different Cu complexes. Somewhat to our surprise, the structures proved that the Halterman substituents, even in conjunction with β-octabromo-substitution, are unable to lock the Cu-corrole conformation into a given chirality. Although in a certain sense such a finding may be considered disappointing, the results shed valuable light on the conformational dynamics of copper corroles. Together with our inability to resolve copper β-octabromo- and β-octakis(trifluoromethyl)- *meso*-triarylcorroles, the present

study underscores the facile interconversion of the *P* and *M* conformations of sterically hindered Cu corroles. Although at this point we have not yet computationally located a transition state for this process, we may speculate that saddling inversion provides a plausible pathway. Finally, there can be no doubt that the present synthesis of Halterman corrole derivatives will open up the study of chiral metallocorroles as asymmetric catalysts, especially for group transfer[24,25,26,27] reactions such as hydroxylation/epoxidation,[28,29,30,31] aziridination,[32,33,34] and cyclopropanation,[35,36,37,38,39] an area where chiral metalloporphyrins already play a significant role.[29,40,41,42]

Experimental Section

Materials and Instruments. All reagents and solvents were used as purchased except pyrrole, which was purified by passing through a pad of basic aluminum oxide 60 (Activity I, 0.063-0.200 mm particle size, Merck Millipore). The Halterman aldehydes (1*S*,4*R*,5*R*,8*S*)-1,2,3,4,5,6,7,8-octahydro-1:4,5:8-dimethanoanthracene-9-carboxaldehyde and its enantiomer as well as the corresponding racemic compound were synthesized as reported.[21] Free-base Halterman corroles were synthesized according to a modified version of Gryko's method employing sterically hindered dipyrromethane.[23] Copper complexes were prepared as previously described.[7] Silica gel 150 (35-70 μm particle size, Davisil) was generally used for column chromatography. Silica gel 60 preparative thin-layer chromatography plates (20 x 20 cm; 0.5 mm thick, Merck) were used for final purification of all compounds. UV-vis spectra were recorded on an HP 8453 spectrophotometer at room temperature in CH_2Cl_2. ECD spectra were recorded on a Jasco J-825 CD spectrometer employing 2-mm quartz cells and metallocorrole solutions in dichloromethane with maximum absorbances in the range 0.8-1.2. Each ECD spectrum was acquired three times and the data were averaged. Proton NMR spectra were recorded on a Mercury Plus Varian spectrometer at 400 MHz in $CDCl_3$ and referenced to residual $CHCl_3$ at δ = 7.26 ppm. High-resolution electrospray ionization (ESI) mass spectra were recorded on an LTQ Orbitrap XL spectrometer.

Common synthetic procedure for 5,10,15-tris[(1*S*,4*R*,5*R*,8*S*)-1,2,3,4,5,6,7,8-octahydro-1:4,5:8-dimethanoanthracen-9-yl]corrole, $H_3[\mathcal{H}^f{}_3Cor]$, its enantiomer, and its racemate. To the Halterman aldehyde (480 mg, 2 mmol) thoroughly dissolved in MeOH (600 mL) was added pyrrole (279 μL, 4 mmol), followed by a solution made from 37% HCl (16.5 mL) diluted in distilled water (300 mL). The resulting mixture was stirred overnight for about

16-17 h. The orange suspension obtained was extracted with $CHCl_3$ and the organic phase was washed twice with distilled water. The olive-green organic phase was dried with anhydrous Na_2SO_4 and filtered. The filtrate was diluted with $CHCl_3$ to a volume of 450 mL and refluxed for 1 h with *p*-chloranil (991 mg, 4 mmol). The suspension obtained was concentrated to a minimum volume and chromatographed on a silica gel column with 1:1 *n*-hexane/CH_2Cl_2 as eluent, yielding the free-base corrole as the first brown band. Yield: 235 mg (38.2%). UV-Vis λ_{max} (nm), ε x 10^{-4} ($M^{-1}cm^{-1}$): 388 (8.83), 399 (8.12), 419 (6.51), 548 (0.80), 703 (0.40). ^{1}H NMR: δ -0.54 to 0.75 (br); 0.92 – 1.19 (br); 1.26 – 1.45 (m, br); 1.74 – 2.20 (m, br). HR-MS (ESI^+, major isotopomer): $[M + H]^+$ = 921.4901 (expt), 921.4891 (calcd). Elemental analysis found (calcd): C, 86.68 (87.16); H, 6.80 (6.77), N, 6.08 (6.07).

Synthesis of copper 5,10,15-tris[(1*S*,4*R*,5*R*,8*S*)-1,2,3,4,5,6,7,8-octahydro-1:4,5:8-dimethanoanthracene-9-yl]corrole, its enantiomer, and its racemate, Cu[$\mathscr{H}_3$Cor]. Copper acetate (4 equiv, 43 mg) was added to a solution of the free-base (50 mg, 0.054 mmol) in 5 mL pyridine. After stirring for 20 min, the suspension was evaporated to a brown residue which was dissolved in a minimum volume of $CHCl_3$ and eluted through a silica gel column with 7:3 *n*-hexane/CH_2Cl_2. The copper corrole was eluted as brown bands. Yield: 47 mg (88.5 %). UV-Vis λ_{max} (nm), ε x 10^{-4} ($M^{-1}cm^{-1}$): 411 (7.84), 541 (0.90), 653 (0.20). ^{1}H NMR: δ 0.81 – 0.87 (m, 3 H, CH_2); 0.92 – 1.01 (m, 3 H, CH_2); 1.15 – 1.21 (m, 6 H, CH_2); 1.35 (d, 2 H, CH_2); 1.39 (d, 2 H, CH_2); 1.44 (d, 2 H, CH_2); 1.62 – 1.73 (m, 9 H, CH_2); 1.77 – 1.88 (m, 9 H, CH_2); 2.98 (br s, 2 H, CH); 3.09 (br s, 2 H, CH); 3.27 (br s, 2 H, CH); 3.37 (br d, 4 H, CH); 3.42 (br d, 2 H, CH); 7.02 (d, 2 H, β-H); 7.04 (s,1 H, *p*-H); 7.09 (s, 2 H, *p*-H); 7.22 (br s, 2H); 7.39 (br d, 2 H, β-H); 8.01 (br s, 2 H, β-H). HR-MS (ESI^+, major isotopomer): $[M]^+$ = 982.4044 (expt), 982.4030 (calcd). Elemental analysis found (calcd): C, 81.10 (81.80); H, 5.86 (6.04); N, 5.32 (5.70).

Synthesis of copper 2,3,7,8,12,13,17,18-octabromo-5,10,15-tris(1,2,3,4,5,6,7,8-octahydro-1:4,5:8-dimethanoanthracen-9-yl]corrole, Cu[Br$_8$$\mathscr{H}_3$Cor]. The Cu[$\mathscr{H}_3$Cor] starting material (30 mg, 0.03 mmol) was dissolved in $CHCl_3$ (15 mL) and to the solution was added Br_2 (2.44 mmol, 125µL, 80 equiv), dissolved in $CHCl_3$ (10 mL), in a dropwise manner over 20 min. The resulting suspension was stirred for 1 h, following which pyridine (203 μL, 2.52 mmol, 84 equiv) dissolved in $CHCl_3$ (10 mL) was added dropwise over 20 min. The resulting mixture was again stirred for 1 h and then shaken with an equal volume of 20% w/v aqueous $Na_2S_2O_7$. The organic phase was then dried over anhydrous Na_2SO_4, filtered, and evaporated to a

minimum. Column chromatography on silica gel with 13:7 *n*-hexane/CH_2Cl_2 resulted in brown bands, which were combined and evaporated to yield the crude product, which was further purified by crystallization from 1:1 $CH_3OH/CHCl_3$. Yield: 30 mg (62%). UV-Vis λ_{max} (nm), ε x 10^{-4} ($M^{-1}cm^{-1}$): 411 (5.54), 457 (7.52), 547 (1.47), 651 (0.72). ^{1}H NMR: δ 1.07 – 1.18 (m, 6H, CH_2); 1.21 –1.36 (m, 8 H, CH_2); 1.39 (d, 2 H, CH_2); 1.42 – 1.48 (m, 4 H, CH_2); 1.57 – 1.65 (m, 3 H, CH_2); 1.74 – 1.94 (m, 11 H, CH_2); 2.03 (d, 2 H, CH_2); 2.65 (bd, 2 H, CH); 2.83 (bd, 2 H, CH); 3.20 (br d, 2 H, CH); 3.27 (br d, 2 H, CH); 3.33 (br d, 2 H, CH); 3.36 (br d, 2 H, CH); 7.15 (s,1 H, *p*-H); 7.21 (s, 2 H, *p*-H). HR-MS (ESI^+, major isotopomer): $[M]^+$ = 1613.6810 (expt), 1613.6805 (calcd). Elemental analysis found (calcd) : C 49.41 (49.83), H, 2.98 (3.18), N 3.66 (3.47).

X-ray structure determination. X-ray data for all three crystalline materials were collected on beamline 11.3.1 at the Advanced Light Source, employing a Bruker D8 diffractometer equipped with a PHOTON100 CMOS detector operating in shutterless mode. The crystal was coated in protective oil prior to being mounted on a MiTeGen® kapton micromount and placed under a nitrogen stream at 100(2) K provided by an Oxford Cryostream 800 Plus low temperature apparatus. Diffraction data were collected using synchrotron radiation monochromated with Si(111) to a wavelength of 0.7749(1)Å. An approximate full-sphere of data was collected using a combination of phi and omega scans; multiple spheres of data were collected for Cu[$\mathscr{H}_3$Cor] and Cu[$Br_8\mathscr{H}_3$Cor] to ensure that the absolute configuration could be reliably determined from anomalous scattering. The structures were solved by intrinsic phasing (SHELXT)[43] and refined by full-matrix least squares on F^2 (SHELXL-2014).[44] All non-hydrogen atoms were refined anisotropically. Hydrogen atoms were geometrically calculated and refined as riding atoms. Some disorder of the pendant groups was observed for Cu[$\mathscr{H}_3$Cor] and Cu[$Br_8$5,15-$\mathscr{H}_2$-10-$\mathscr{H}$Cor], and these have been modelled over multiple sites. SQUEEZE analysis was used to determine the solvent content of the voids in Cu[$Br_8$5,15-$\mathscr{H}_2$-10-$\mathscr{H}$Cor], as the solvent of crystallization was too disordered for modeling attempts. Additional crystallographic information has been summarized in Tables 1 to 4 and full details can be found in the crystallographic information files provided as Supporting Information.

Acknowledgements. The above work was supported by grants 231086 and 262229 of the Research Council of Norway. This research also used resources of the Advanced Light Source,

which is a DOE Office of Science User Facility under contract no. DE-AC02-05CH11231. We thank Dr. Soizic Chevance for stimulating discussions and recording the CD spectra.

References

[1] Moscowitz, A. Theoretical Aspects of Optical Activity. Part 1: Small Molecules. *Adv. Chem. Phys*. **1962**, *4*, 67-112.

[2] Kwit, M.; Skowronek, P.; Gawronski, J.; Frelek, J.; Woznica, M.; Butkiewicz, A. In *Comprehensive Chiroptical Spectroscopy*, Vol. 2, *Applications in Stereochemical Analysis of Synthetic Compounds, Natural Products, and Biomolecules.* Berova, N.; Polavarapu, P. L.; Nakanishi, K.; Woody, R. W. (eds.), Wiley, New York, 2012, Ch. 2, pp. 39-72.

[3] Mislow, K.; Siegel, J. Stereoisomerism and Local Chirality. *J. Am. Chem. Soc.* **1984**, *106*, 3319-3328.

[4] She, Y.; Chen, C.-F. Helicenes: Synthesis and Applications. *Chem. Rev.* **2012**, *112*, 1463–1535.

[5] Thilgen, C.; Gosse, I.; Diederich, F. Chirality in Fullerene Chemistry. *Top. Stereochem*. **2003**, *23*, 1-124.

[6]. Ghosh, A. Electronic Structure of Corrole Derivatives: Insights from Molecular Structures, Spectroscopy, Electrochemistry, and Quantum Chemical Calculations. *Chem. Rev*. **2017**, *117*, 3798–3881.

[7]. Wasbotten, I. H.; Wondimagegn, T.; Ghosh, A. Electronic Absorption, Resonance Raman, and Electrochemical Studies of Planar and Saddled Copper(III) *Meso*-Triarylcorroles. Highly Substituent-Sensitive Soret Bands as a Distinctive Feature of High-Valent Transition Metal Corroles. *J. Am. Chem. Soc.* **2002,** *124*, 8104-8116.

[8] Ou, Z.; Shao, J.; Zhao, H.; Ohkubo, K.; Wasbotten, I. H.; Fukuzumi, S.; Ghosh, A.; Kadish, K. M. Spectroelectrochemical and ESR Studies of Highly Substituted Copper Corroles. *J. Porphyrins Phthalocyanines* **2004,** *8*, 1236-1247.

[9] Bröring, M.; Bregier, F.; Tejero E. C.; Hell, C.; Holthausen M. C. Revisiting the Electronic Ground State of Copper Corroles. *Angew. Chem., Int. Ed.* **2007**, *46*, 445–448.

[10] Thomas, K. E.; Alemayehu, A. B.; Conradie, J.; Beavers, C.; Ghosh, A. Synthesis and Molecular Structure of Gold Triarylcorroles. *Inorg. Chem.* **2011**, *50*, 12844–12851.

[11] Berg, S.; Thomas, K. E.; Beavers, C. M.; Ghosh, A. Undecaphenylcorroles. *Inorg. Chem.* **2012,** *51*, 9911-9916.

[12] Thomas, K. E.; Beavers, C. M.; Ghosh, A. Molecular Structure of a Gold *β*-Octakis(trifluoromethyl)-*meso*-triarylcorrole: An 85° Difference in Saddling Dihedral Relative to Copper. *Mol. Phys*. **2012**, *110*, 2439-2444.

[13] Alemayehu, A. B.; Hansen, L. K.; Ghosh, A. Nonplanar, Noninnocent, and Chiral: A Strongly Saddled Metallocorrole. *Inorg. Chem.* **2010,** *49*, 7608-7610.

[14] Thomas, K. E.; Vazquez-Lima, H.; Fang, Y.; Song, Y.; Gagnon, K. J.; Beavers, C. M.; Kadish, K. M.; Ghosh, A. Ligand Noninnocence in Coinage Metal Corroles: A Silver Knife-Edge. *Chem. - Eur. J.* **2015,** *21*, 16839-16847.

[15] Thomas, K. E.; Wasbotten, I. H.; Ghosh, A. Copper *β*-Octakis(Trifluoromethyl)Corroles: New Paradigms for Ligand Substituent Effects in Transition Metal Complexes. *Inorg. Chem.* **2008,** *47*, 10469-10478.

[16] Thomas, K. E.; Conradie, J.; Hansen, L. K.; Ghosh, A. A Metallocorrole with Orthogonal Pyrrole Rings. *Eur. J. Inorg. Chem.* **2011**, 1865–1870.

[17] Schies, C.; Alemayehu, A. B.; Vazquez-Lima, H.; Thomas, K. E.; Bruhn, T.; Bringmann, G.; Ghosh, A. Metallocorroles as Inherently Chiral Chromophores: Resolution and Electronic Circular Dichroism Spectroscopy of a Tungsten Biscorrole. *Chem. Commun*. **2017**, *53*, 6121-6124.

[18] Alemayehu, A. B.; Vazquez-Lima, H.; McCormick, L. J.; Ghosh, A. Relativistic Effects in Metallocorroles: Comparison of Molybdenum and Tungsten Biscorroles. *Chem. Eur. J*. **2016**, *22*, 6914-6920.

[19] Alemayehu, A. B.; Vazquez-Lima, H.; Gagnon, K. J.; Ghosh, A. Tungsten Biscorroles: New Chiral Sandwich Compounds. *Chem. Eur. J*. **2016**, *22*, 6914-6920.

[20]. For an example of a chiral corrole derivative that, however, is not an inherently chiral chromophore, see: Gross, Z.; Galili, N. *N*-Substituted Corroles: A Novel Class of Chiral Ligands. *Angew. Chem. Int. Ed*. **1999**, *38*, 2366–2369.

[21] Halterman, R. L.; Jan, S. T. Catalytic Asymmetric Epoxidation of Unfunctionalized Alkenes Using the First D_4-Symmetric Metallotetraphenylporphyrin. *J. Org. Chem.* **1991**, *56*, 5253-5254.

[22] Halterman, R. L., Mei, X. Synthesis of D_2-Symmetric 5,10,15,20-Tetraarylporphyrins from C_2-Symmetric Benzaldehydes and Achiral Aryldipyrromethanes. *Tetrahedron Letters*. **1996**, *37*, 6291-6294.

[23] Koszarna, B.; Gryko, D. T. Efficient Synthesis of *meso*-Substituted Corroles in a H_2O−MeOH Mixture. *J. Org. Chem*. **2006**, *71*, 3707-3717.

[24] Halterman, R. L.; Jan, S-T, Nimmons, H. L.; Standlee, D. J.; Khan, M. A. Synthesis and Catalytic Reactivity of D_4-Symmetric Dinorbornabenzene-derived Metallotetraarylporphyrins. *Tetrahedron* **1997**, *53*, 11257-11276.

[25] Wang, J-C.; Zhang, Y.; Xu, Z-J.; Lo, V. K-Y.; Che, C-M. Enantioselective Intramolecular Carbene C–H Insertion Catalyzed by a Chiral Iridium(III) Complex of D_4-Symmetric Porphyrin Ligand. *ACS Catal*. **2013**, *3*, 1144–1148.

[26] Thu, H-Y.; Tong, G. S-M.; Huang, J-S.; Chan, S. L-F.; Deng, Q-H.; Che, C-M. Highly Selective Metal Catalysts for Intermolecular Carbenoid Insertion into Primary C−H Bonds and Enantioselective C−C Bond Formation. *Angew. Chem. Int. Ed*. **2008**, *47*, 9747-9751.

[27] Nicolas, I.; Chevance, S.; Le Maux, P.; Simonneaux, G. Chiral Recognition of Amines and Amino Acid Derivatives by Optically Active Ruthenium Halterman Porphyrins in Organic Solvents and Water. *Tetrahedron: Asymmetry* **2010**, *21*, 1788-1792.

[28] Halterman, R. L.; Jan, S-T.; Abdulwali, A.H.; Standlee, D. J. Synthesis and Catalytic Reactivity of Sterically and Electronically Modified D_4-Symmetric Metallotetraarylporphyrins. *Tetrahedron* **1997**, *53*, 11277-11296.

[29] Berkessel, A.; Kaiser, P.; Lex, J. Electronically Tuned Chiral Ruthenium Porphyrins: Extremely Stable and Selective Catalysts for Asymmetric Epoxidation and Cyclopropanation. *Chem. Eur. J*. **2003**, *9*, 4746-4756.

[30] Amiri, N.; Le Maux, P.; Srour, H.; Nasri, H.; Simonneaux, G. Nitration of Halterman Porphyrin: a New route for Fine-tuning Chiral Iron and Manganese Porphyrins with Application in Epoxidation and Hydroxylation reactions using Hydrogen Peroxide as Oxidant. *Tetrahedron* **2014**, *70*, 8836-8842.

[31] Srour, H.; Le Maux, P.; Simmoneax, G. Enantioselective Manganese-Porphyrin-Catalyzed Epoxidation and C-H hydroxylation with Hydrogen Peroxide in Water/Methanol Solutions. *Inorg. Chem*. **2012**, *51*, 5850-5856.

[32] Jones, J. E.; Ruppel, J. V.; Gao, G.-Y.; Moore, T. M.; Zhang, X. P. Cobalt-Catalyzed Asymmetric Olefin Aziridination with Diphenylphosphoryl Azide. *J. Org. Chem*. **2008**, *73*, 7260–7265.

[33] Subbarayan, V.; Ruppel, J. V.; Zhu, S.; Perman, J. A.; Zhang, X. P. Highly Asymmetric Cobalt-Catalyzed Aziridination of Alkenes with Trichloroethoxysulfonyl Azide ($TcesN_3$). *Chem. Commun*. **2009**, 4266-4268

[34] Jiang, H.; Lang, K.; Lu, H.; Wojtas, L.; Zhang, X. P. Asymmetric Radical Bicyclization of Allyl Azidoformates via Cobalt(II)-Based Metalloradical Catalysis. *J. Am. Chem. Soc*. **2017**, *139*, 9164–9167.

[35] Lai, T-S.; Chan, F-Y.; So, P-K.; Ma, D-L.; Wong, K-Y.; Che, C-M. Alkene Cyclopropanation Catalyzed by Halterman Iron Porphyrin: Participation of Organic Bases as Axial Ligands. *Dalton Trans*. **2006**, 4845-4851.

[36] Che, C. M.; Huang, J. S.; Lee, F. W.; Li, Y.; Lai, T. S.; Kwong, H. L.; Teng, P. F.; Lee, W. S.; Lo, W. C.; Peng, S. M.; Zhou, Z. Y. Asymmetric Inter- and Intramolecular Cyclopropanation of Alkenes Catalyzed by Chiral Ruthenium Porphyrins. Synthesis and Crystal Structure of a Chiral Metalloporphyrin Carbene Complex. *J. Am. Chem. Soc.* **2001,** *123*, 4119-4129.

[37] Nicolas, I.; Le Maux, P.; Simonneaux, G. Synthesis of Chiral Water-soluble Metalloporphyrins (Fe, Ru,): New catalysts for Asymmetric Carbene Transfer in Water. *Tetrahedron Lett*. **2008**, *49*, 5793-5795.

[38]. Nicolas, I.; Roisnel, T.; Le Maux, P.; Simonneaux, G. Asymmetric Intermolecular Cyclopropanation of Alkenes by Diazoketones Catalyzed by Halterman Iron Porphyrins. *Tetrahedron Lett*. **2009**, *50*, 5149-5151.

[39] Chen. Y.; Ruppel, J. V.; Zhang, X. P. Cobalt-Catalyzed Asymmetric Cyclopropanation of Electron-Deficient Olefins. *J. Am. Chem. Soc*. **2007**, *129*, 12074–12075

[40]. Rose, E.; Andrioletti, B.; Zriga, S.; Quelquejeu-Ethève, M. Enantioselective epoxidation of olefins with chiral metalloporphyrin catalysts. *Chem. Soc. Rev*. **2005**, *34*, 573-583.

[41] Simonneaux, G.; Le Maux, P.; Chevance, S.; Srour, H. Recent Advances in Catalysis by Water-Soluble Metalloporphyrins. In *Handbook of Porphyrin Science*. Kadish, K. M.; Smith, K. M.; Guilard, R. (eds.). 2012, Vol. 21, pp. 377-410.

[42] Simonneaux, G.; Srour, H.; Le Maux, P.; Chevance, S.; Carrie, D. Metalloporphyrin Symmetry in Chiral Recognition and Enantioselective Catalysis. *Symmetry* **2014**, *6*, 210-221.

[43] Sheldrick, G. M. SHELXT - Integrated Space-Group and Crystal-Structure Determination. *Acta Cryst.* **2015**, *A71*, 3-8.

[44] Sheldrick, G. M. Crystal Structure Refinement with SHELXL. *Acta Cryst.* **2015**, *C71*, 3-8.

For Table of Contents only:

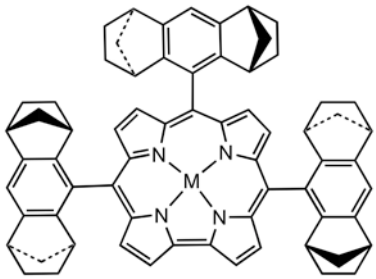

Synopsis: The first Halterman corroles have been synthesized and complexed with copper, affording the first electronic circular dichroism spectra of the inherently chiral copper corrole chromophore. Spectroscopic and crystallographic evidence, however, suggests that the *P* and *M* conformations of the Cu corroles readily interconvert in solution.